Supplementary Information

High Voltage Hybrid Zn-MnO_2/air Batteries via Decoupled Electrolyte

Chengwei Wang [a-c], Jintao Zhang [b], Yanwei Lum [b,c], Ming Liu [a,d], Zhaolin Liu [b*], Bing Li [a*]

a. State Key Laboratory of Space Power-Sources, School of Chemistry and Chemical Engineering, Harbin Institute of Technology, Harbin, Heilongjiang 150001, China

b. Institute of Materials Research and Engineering (IMRE), Agency for Science, Technology and Research (A*STAR), 2 Fusionopolis Way, #08-03 Innovis, Singapore 138634, Republic of Singapore

c. Department of Chemical and Biomolecular Engineering, National University of Singapore, Singapore 117585, Republic of Singapore

d. Engineering Laboratory of Advanced Energy Materials, Ningbo Institute of Materials Technology & Engineering, Chinese Academy of Sciences, Ningbo, Zhejiang 315201, China

Emails: ZL: zl-liu@imre.a-star.edu.sg; BL: bing.li2020@hit.edu.cn;

Experimental section

Materials

Sulfuric acid (AR) was purchased from Tianjin Kemi Ou Chemical Reagent Co., LTD. $MnSO_4 \cdot H_2O$ (AR, ≥99%), K_2SO_4 (AR, ≥99%), KOH (AR, ≥85%) and $Zn(CH_3COOH)_2$ (≥99%) was obtained from Shanghai Aladdin Biochemical Technology Co., LTD. The brand and model of the use of cation exchange membranes (CEM) are Fumasep PKB-PK-130. Similarly, the brand and model of the use of anion exchange membranes (AEM) are Fumasep Paa-3-PK-130. All commercially available chemicals were used as received, without further modifications.

Synthesis of C@Co-N-C electrode

Firstly, the carbon felt electrode was coated with polydopamine (C@PDA), and the coating method has been reported in previous report.[1] Then the ZIF67 was *in-situ* growth on C@PDA, the synthesis method still refers to the reported study.[2] After that, the hybrid electrode was thermally treated in Ar at 900℃ for 30 min to C@Co-N-C, as exhibited in Fig. S1. To determine the mass loading of Co-N-C on the carbon felt (CF), ten CF samples were weighted before and after Co-N-C deposition. The average mass loading was calculated to be 2.3 mg cm^{-2}. Furthermore, the C@Co-N-C electrode features distinct asymmetric wettability. The hydrophobic side prevents electrolyte leakage and helps establish a stable gas-liquid-solid interface for the ORR, while the hydrophilic side allows the electrolyte to contact with C@Co-N-C catalyst and carbon felt fiber to facilitate electrochemical reactions. This functional design was achieved via a two-step treatment. 1) The back surface was coated with a mixture of 10% PTFE and 2.5% active carbon (AC) by air spraying (PTFE loading: ~ 10 mg cm^{-2}). Subsequent annealing at 300°C for 2 h under nitrogen led to a superhydrophobic back surface with a contact angle >150° (Fig. S3a,b). And 2) O_2 plasma treatment (100 W, 2 min) rendered the electrode hydrophilic, evidenced by the rapid permeation of water droplets (Fig. 3Sc,d) during contact angle measurements.

Battery fabrication

The Zn-MnO_2/air battery was consisted of three chambers separated by CEM and

AEM that consist of three chambers, each with a different electrolyte, the anode alkaline chamber (6 M KOH / 0.2 M $Zn(CH_3COO)_2$), the cathode acidic chamber (3 M H_2SO_4 / 1 M $MnSO_4$), and the neutral chamber (0.5 M K_2SO_4) that separates the two electrode chambers. The volume of electrolyte in each chamber is 6 mL. The Zn plate as anode and the synthesized multi-functional electrode as cathode, respectively. A customized acrylic mold is used as the overall structure of the battery, silicone pads are used for sealing, and bolts and nuts are used as fasteners for the battery. The multi-function cathode has a thickness of 2 mm, where one side interfaces with the electrolyte while the other interfaces with air, each side possessing a contact area of 1 cm^{-2}. For the decoupled electrolyte Zn-MnO_2 battery, the assembly method aligns with that of the Zn-MnO_2/air battery, except for the sealing of the electrodes in the electrolyte to isolate them from the ambient air. Unless specified, the Zn-MnO_2 battery referred to in the text specifically refers to the decoupled electrolyte Zn-MnO_2 battery.

Characterizations

The morphology images were observed from the scanning electron microscope (SEM, TESCAN AMBER, The Czech Republic) equipped with an energy-dispersive X-ray spectrometer (EDS) to investigate the surface element compositions of the materials. X-ray diffraction (XRD) patterns were conducted by Model D8 Avance X-ray diffractometer (Bruker, Germany) with Cu Ka radiation (λ = 0.15418 nm). Raman spectroscopy was measured by a RENISHAW Raman spectrometer with a laser wavelength of 532 nm. The elemental valence states of the electrode were determined using X-ray photoelectron spectroscopy (XPS) on Thermo Fisher, ESCALAB250Xi.

Electrochemical Measurements

The evaluated cyclic voltammetry (CV) curves and and linear sweep voltammetry (LSV) curves of the batteries were tested in an electrochemical workstation (CHI 660E, CH Instrument), the charge and discharge curves (GCD) were measured in the NEWARE battery test system. For Zn-MnO_2/air battery, during the performance evaluation of the Zn-air cell, the potential window testing range for CV and LSV curves is 1.2 to 2.7 V, while for the hybrid batteries, it is 1.2 to 3.0 V, as at 3.0 V potential, Mn^{2+} oxidizes to MnO_2. Additionally, for both the hybrid Zn-MnO_2/air battery and the

Zn-MnO_2 battery, the charging potential during charge and discharge testing is set at 3.0 V. In the case of the Zn-MnO_2 battery, the discharge cutoff voltage is set at 1.0 V.

Calculation Method

In the decoupled electrolyte Zn-MnO_2 battery, the electrochemical reactions occur as following:

$$\text{Anode:}\quad Zn + 2OH^- - 2e^- \rightleftharpoons ZnO + H_2O \qquad (E^\theta = -1.25\ \text{V } \textit{vs.}\ \text{SHE}) \tag{1}$$

$$ZnO + H_2O + 2OH^- \rightleftharpoons Zn(OH)_4^{2-} \tag{2}$$

$$\text{Cathode:}\ MnO_2 + 4H^+ + 2e^- \rightleftharpoons Mn^{2+} + 2H_2O \qquad (E^\theta = 1.224\ \text{V } \textit{vs.}\ \text{SHE}) \tag{3}$$

According to Nernst equation, the electrode potential of cathode (E_C) and anode (E_A) can be calculated by following equations:

$$E_{C(MnO_2)} = E^{\theta}_{Mn^{2+}/MnO_2} + \frac{RT}{nF} ln \frac{\alpha_{MnO_2}\alpha_{l}}{\alpha_{Mn^{2+}}\alpha} \tag{4}$$

$$E_A = E^{\theta}_{ZnO/Zn} + \frac{RT}{nF} ln \frac{\alpha_{ZnO}\alpha_{H_2O}}{\alpha_{Zn}\alpha^{2}_{OH^-}} \tag{5}$$

For the decoupled electrolyte Zn-air battery, the anode reaction is consistent with the Zn-MnO_2 battery, with the cathode reaction equation as follows:

$$O_2 + 4H^+ + 4e^- \rightleftharpoons 2H_2O \ (E^\theta = 1.23\ \text{V } \textit{vs.}\ \text{SHE}) \tag{6}$$

The cathode voltage of Zn-air battery is calculated as follows:

$$E_{C(air)} = E^{\theta}_{O_2/H_2O} + \frac{RT}{nF} ln \frac{(P_{O_2}/P^\theta)\alpha^{4}_{H^+}}{\alpha^{2}_{H_2O}} \tag{7}$$

Considering the potential difference on both sides of the ion exchange membrane, it is necessary to calculate the transmembrane potential to correct the theoretical voltage of decoupled electrolyte Zn-MnO_2 battery. The transmembrane potential across the CEM is determined by the K^+ concentration, whereas the transmembrane potential across the AEM is contingent upon the SO_4^{2-} concentration, as follows:[3,4]

$$E_{CEM} = \frac{RT}{nF} ln \frac{2\alpha_{K_2SO_4}}{\alpha_{KOH}} \quad (8)$$

$$E_{AEM} = \frac{RT}{nF} ln \frac{\alpha_{H_2SO_4} + \alpha_{MnSO_4}}{\alpha_{K_2SO_4}} \quad (9)$$

Where R (8.3144 J K^{-1} mol^{-1}) is the value of gas constant, T (298 K) is temperature, n is the electron transfer number, and F (96.487 kJ V^{-1} mol^{-1}) is Faraday's constant. In the ideal solution, the activity value of solids and liquids are considered as 1 and the ions activity values are the corresponding concentration values. The partial pressure of oxygen is 21% of atmospheric pressure. The concentration of H_2SO_4 ranges from 0.1 to 4 M, the concentration of $MnSO_4$ is 1 M, and the concentration of K_2SO_4 is 0.5 M. Eventually, the theoretical voltage calculation method for the Zn-MnO_2 battery could be calculated as following equation, and the detailed values are showed in Table 1.

$$E = (E_C + E_{CEM}) - (E_{AEM} + E_A) \quad (10)$$

Table S1 Theoretical voltage of Zn-MnO_2 and Zn-air batteries at different H_2SO_4 concentrations

H_2SO_4 (M)	**Zn-MnO_2 E (V)**	**Zn-air E (V)**	**H_2SO_4 (M)**	**Zn-MnO_2 E (V)**	**Zn-air E (V)**
0.1	2.576	2.537	2.0	2.744	2.629
0.3	2.634	2.568	2.5	2.758	2.637
0.5	2.663	2.583	3.0	2.769	2.643
1.0	2.702	2.605	3.5	2.778	2.649
1.5	2.726	2.619	4.0	2.787	2.653

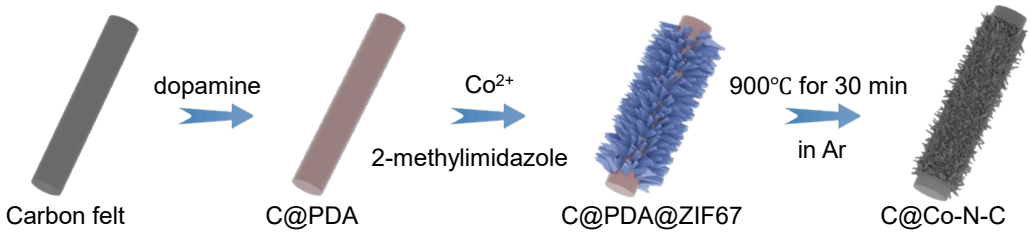

Fig. S1 Schematic illustration of C@Co-N-C electrode preparation.

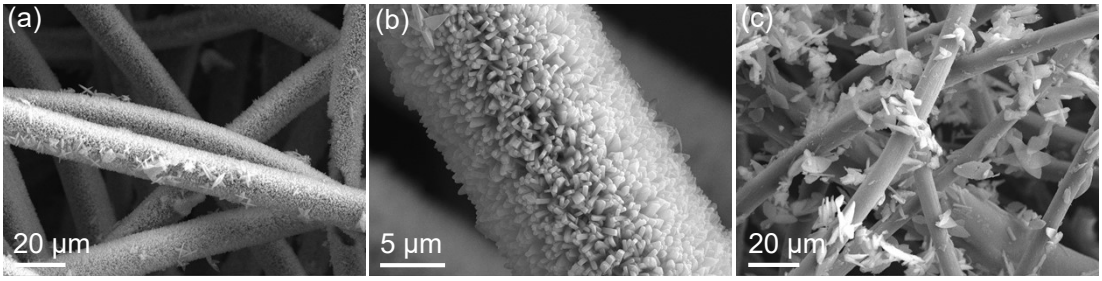

Fig. S2 (a, b) SEM images of *in-situ* growth of ZIF67 on carbon felt after PDA modification (C@PDA@ZIF67); (c) SEM image of *in-situ* growth of ZIF67 on carbon felt without PDA modification.

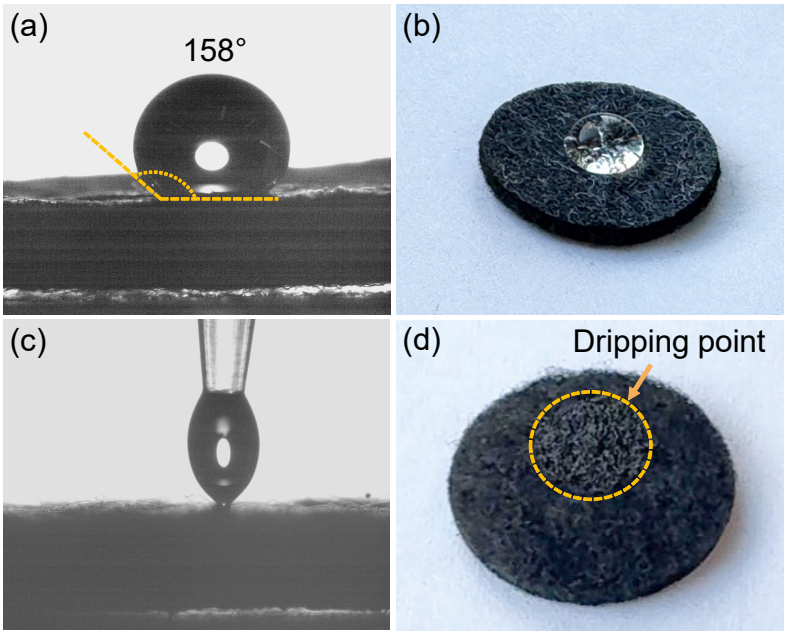

Fig. S3 (a) Contact angle tests of hydrophobic surface of C@Co-N-C; (b) Photograph of the water droplet test on the hydrophobic surface of Co-N-C; (c) Contact angle tests of hydrophilic surface of C@Co-N-C; (d) Photograph of the water droplet test on the hydrophilic surface of Co-N-C.

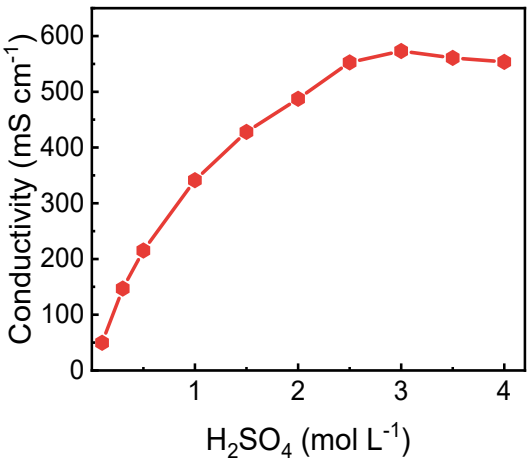

Fig. S4 The electrolyte conductivity under different H_2SO_4 concentrations range from 0.1 ~ 4 M.

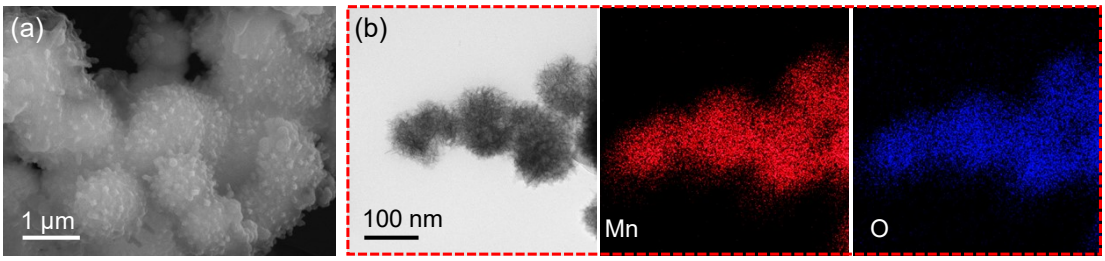

Fig. S5 (a) SEM image of MnO_2; (b) TEM image and elemental mappings of Mn and O.

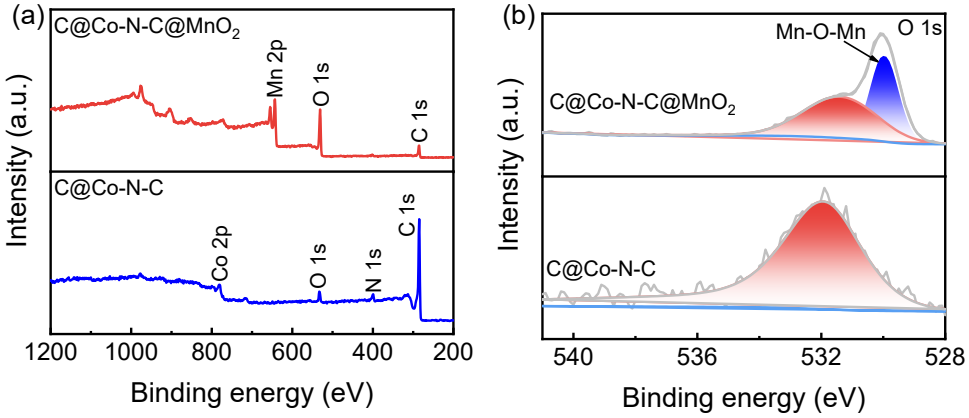

Fig. S6 XPS spectra comparison of C@Co-N-C@MnO_2 and C@Co-N-C. (a) A survey scan; (b) O 1s.

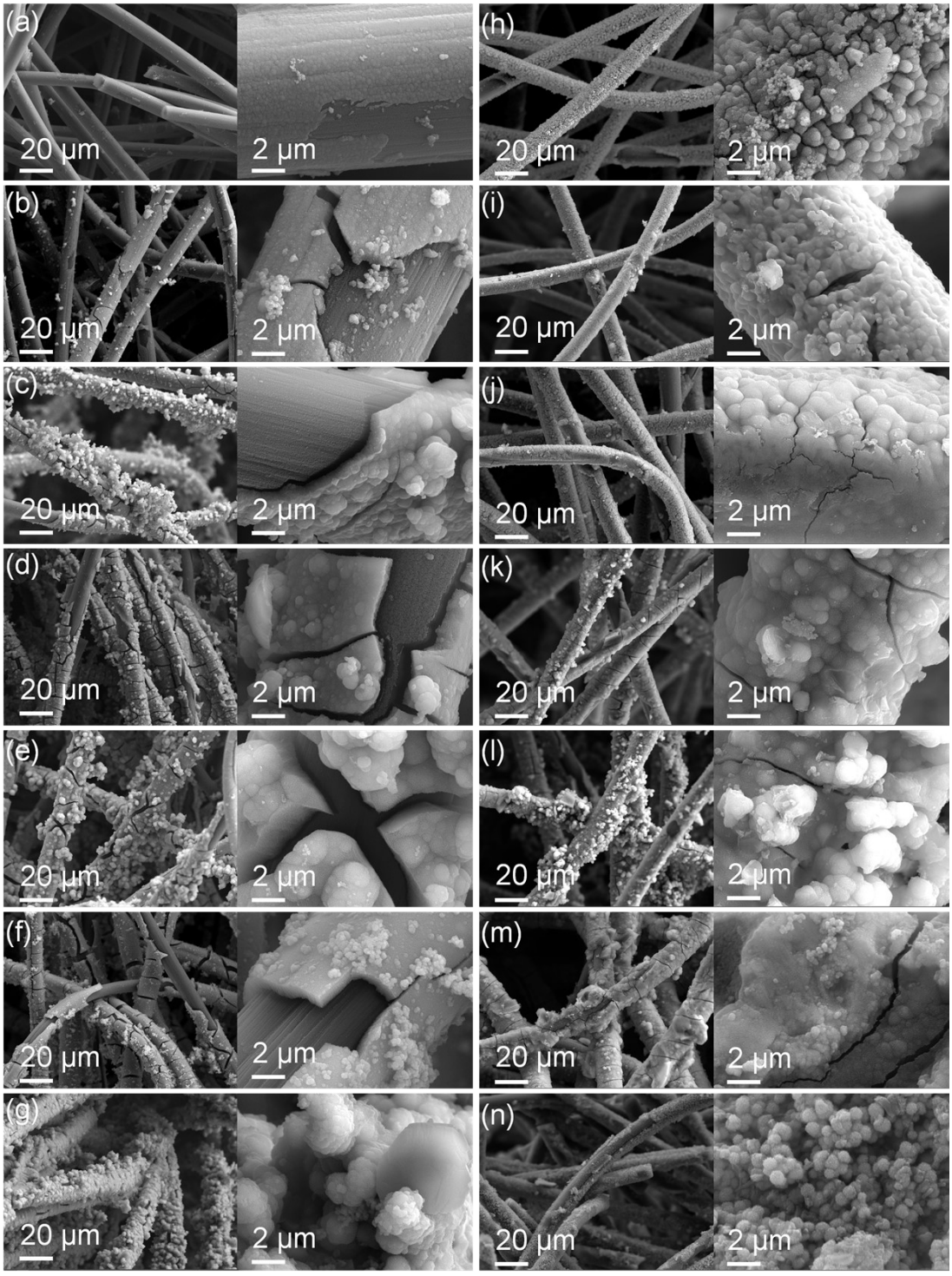

Fig. S7 SEM comparison images of carbon felt (a-g) and Co@Co-N-C (h-n) electrode surface with deposition of MnO_2 at different charging capacities; (a, h) 5 mAh cm^{-2}; (b, i) 10 mAh cm^{-2}; (c, j) 15 mAh cm^{-2}; (d, k) 20 mAh cm^{-2}; (e, l) 25 mAh cm^{-2}; (f, m) 30 mAh cm^{-2}; (g, n) 35 mAh cm^{-2}.

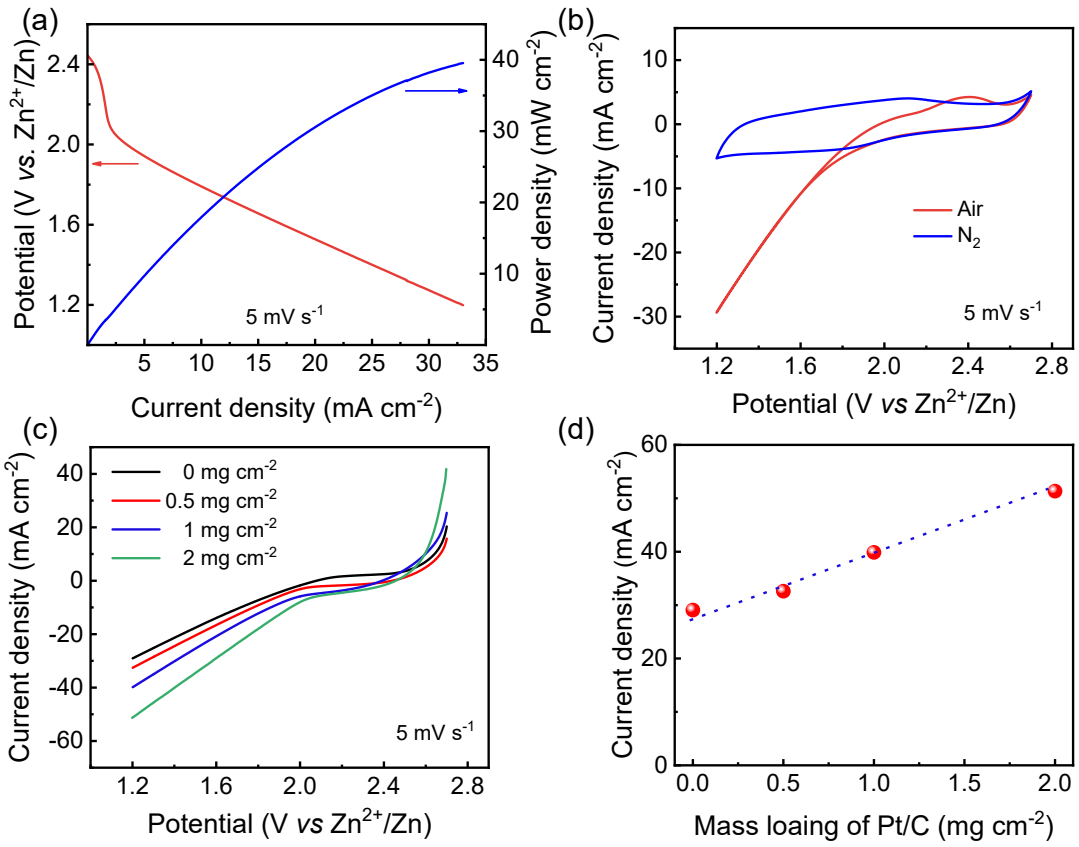

Fig. S8 (a) Electrochemical performance of decoupled electrolyte Zn-air battery. (a) LSV curve and power density with C@Co-N-C electrode; (b) CV curves for air and nitrogen atmospheres without deposition of MnO_2; (c) LSV curve of decoupled electrolyte Zn-air battery using different mass loading of Pt/C catalyst (0.5 ~ 2 mg cm^{-2}); (d) The current densities at different Pt/C loading at 1.2 V estimated according to the LSV curves in (c).

Table S2 Summary of output voltage and areal capacity of Zn-MnO_2 based batteries on reported studies

Areal capacity (mAh cm^{-2})	Voltage (V)	Current density	Electrolyte	Anode	Cathode	Ref.
175	2.63	2 mA cm^{-2}	6 KOH + 0.2 $Zn(Ac)_2$ // 0.5 M K_2SO_4 // 3 M H_2SO_4 + 1 M $MnSO_4$	zinc plate	carbon felt	This work
1	2.44	1 C	3 M NaOH + 0.3 M ZnO // 3 M $MnSO_4$ + 0.3M H_2SO_4 + 0.06M $NiSO_4$	Zn@carbon-felt	carbon felt	5
16	2.25	2 mA cm^{-2}	2.4 M KOH + 0.1 M $Zn(CH_3COO)_2$ // 0.5 M H_2SO_4 + 1.0 M $MnSO_4$	Zn foil	carbon cloth	6
0.48	1.84	2.5 mA cm^{-2}	2.4 M KOH + 0.1 M $Zn(CH_3COO)_2$ // 1.0 M H_2SO_4, 0.3 M $CuSO_4$ + 1.0 M $MnSO_4$	Zn foil	Cu BPE	7
0.35	1.8	2 mA cm^{-2}	2 M $ZnSO_4$ + 0.005 M $MnSO_4$	Zn foil	MnO_2/CNTs foam	8
2.75	1.92	10 mA cm^{-2}	1 M $ZnSO_4$ + 1 M $MnSO_4$	Zn foil	carbon cloth	9
50	1.4	20 mA cm^{-2}	1 M $Zn(Ac)_2$ + 1 M $Mn(Ac)_2$ + 2 M KCl+0.1 M KI	zinc plate	carbon felt	10
1.2	1.4	1 mA cm^{-2}	2 M $ZnSO_4$ + 0.1 M $MnSO_4$	zinc plate	α-MnO_2/CNT	11
15	1.98	13.3 mA cm^{-2}	1 M $MnSO_4$ + 1 M $ZnSO_4$ + 0.2 M H_2SO_4 + 0.05 M $ZnBr_2$ + 0.2 M Br_2	Zn foil	carbon felt	12
9	1.85	10 mA cm^{-2}	1 M $MnSO_4$ + 1 M $ZnSO_4$ + 0.075 M ZnI_2	Zn foil	carbon felt	13
12.08	0.85	2 mA cm^{-2}	2 M $ZnSO_4$ + 0.1 M $MnSO_4$	Zn foil	MnO_2/Cu-Ti foam	14
8	1.3	N/A	3 M $Zn(ClO_4)_2$	Zn	α-MnO_2	15
18	2.05	20 mA cm^{-2}	0.5 M $ZnSO_4$ + 1 M LiTFSI // 1 M $MnSO_4$ + 1 M HTFSI	Zn foil	carbon paper	16
13.3	1.4	40 mA cm^{-2}	0.5 M $Mn(Ac)_2$ + 0.5 M $Zn(Ac)_2$ + 2 M KCl	graphite felt	graphite felt	17
0.99	1.75	0.5 mA cm^{-2}	2 M $ZnCl_2$ + 0.07 M $Mn(H_2PO_4)_2$	Zn foil	Graphite foil	18
5	1.9	8 mA cm^{-2}	0.1 M H_2SO_4 + 1 M $ZnSO_4$ + 1 M $MnSO_4$ + 2 mg	Zn@Pb-Ad	graphite felt	19

			$Pb(OAc)_2$			
2.6	1.92	1 mA cm^{-2}	BF_4-SO_4-1.5	Zn foil	carbon cloth	20
3.54	1.3	1 mA cm^{-2}	2.0 M $ZnSO_4$+0.4 M $MnSO_4$	Zn nanosheets	$K_{0.133}MnO_2$	21
77	2	10 mA cm^{-2}	1 M $ZnSO_4$ + 1 M NaAc + 1 M HAc//1 M $MnSO_4$ + 0.5 M H_2SO_4 + 1 M Na_2SO_4 + 0.15 M $FeSO_4$	zinc plate	carbon felt	22
40	1.5	20 mA cm^{-2}	0.5 M $Mn(Ac)_2$ +0.5 M $Zn(Ac)_2$ + 2 M KCl	zinc plate	CNT/ CF-700	23
88	1.7	20 mA cm^{-2}	2 M $ZnSO_4$ + 1 M Na_2SO_4 // 2 M $MnSO_4$ + 1 M Na_2SO_4 + 0.2M H_2SO_4 + 50 mM $VOSO_4$	zinc foil	3DGAs	24
9	1.91	20 mA cm^{-2}	3 M $ZnCl_2$ + 1 M $Zn(Ac)_2$ + 1M HAc // 1 M $MnCl_2$ + 0.2 M HCl + 4 M $MgCl_2$	graphite plates	graphite plates	25
2	1.95	2 mA cm^{-2}	1 M $ZnSO_4$ + 1 M $MnSO_4$ + 0.1 M H_2SO_4	Zn foam	carbon cloth	26
14.5	1.95	1 C	1 M $MnSO_4$ + 1 M $ZnSO_4$ + 0.1 M H_2SO_4 + 0.05 HPD	zinc foil	carbon felt	27
46.9	1.9	50 mA cm^{-2}	0.05 M H_2SO_4 + 1 M $ZnSO_4$ + 0.5 M $MnSO_4$ + Al-HQ	Zn foil	graphite felt	28
18.9	1.95	20 mA cm^{-2}	1 M $MnSO_4$ + 1 M $ZnSO_4$ + x mg/ml SiO_2 + y M $FeSO_4$ + 0.1 M H_2SO_4	Zn foil	carbon felt	29

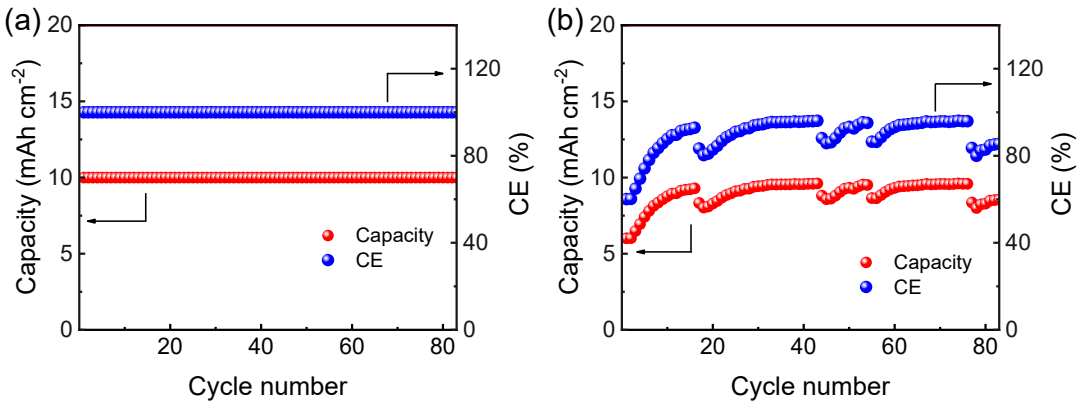

Fig. S9 (a) Cycle stability of hybrid Zn-MnO_2/air battery; (b) Cycle stability of Zn-MnO_2 battery.

Table S3 Comparison of cycle stability of Zn-MnO_2 batteries in recent reports

Batteries	Cycle number	Current density	Capacity retention rate (%)	Electrolyte	Cathode	Ref.
Zn-MnO_2/air	83	5 mA cm^{-2}	100	6 KOH + 0.2 $Zn(Ac)_2$ // 0.5 M K_2SO_4 // 3 M H_2SO_4 + 1 M $MnSO_4$	carbon felt	This work
Zn-MnO_2	2000	2 A g^{-1}	93.8	PU-EG+DMPA-Zn	MnO_2	30
flexible Zn-MnO_2	100	1A g^{-1}	99	PVA-$ZnSO_4$-$MnSO_4$	CC@CNF_1/ CNT_2-MnO_2	31
flexible Zn-MnO_2	100	0.8C	70	$K_{3.6}S_1A_{20}$/$Zn(TFSI)_2$ + LiTFSI	MnO_2@CC	32
Zn-MnO_2	14000	5A g^{-1}	87	2 M $ZnSO_4$ + 0.2 M $MnSO_4$	P-MnO_2	33
quasi-solid-state Zn-MnO_2	>1000	10 A g^{-1}	99.1	PAMPS/PAM	δ-MnO_2	34
Zn-MnO_2	1000	5 A g^{-1}	83	2 M $ZnSO_4$ + 0.2 M $MnSO_4$	EDB@MnO_2	35
Zn-MnO_2	2000	4A g^{-1}	~100	EG–PUA/PAM	CACO-δ-MnO_2	36
Zn-MnO_2	1000	2 A g^{-1}	90.7	BE + $MnSO_4$ + SNC	MnO_2/CNT	37
Zn-MnO_2	1500	1C	94	1 M $MnSO_4$ + 1 M $ZnSO_4$ + 0.1 M H_2SO_4 + 0.05 M HPD	carbon felt	27

Zn-MnO_2	5000	5 mA cm^{-2}	90	H_2O + DMSO + SL	graphite felt	38

Table S4 Comparison of cycle stability of Zn-air batteries in recent reports

Batteries	**Cycle time (h)**	**Current density (mA cm^{-2})**	**Electrolyte**	**Cathode**	**Ref.**
Zn-MnO_2/air	278	5	6 KOH + 0.2 $Zn(Ac)_2$ // 0.5 M K_2SO_4 // 3 M H_2SO_4 + 1 M $MnSO_4$	carbon felt	This work
quasi-solid-state Zn-air	337	1	6 M KOH + 0.2 M $Zn(Ac)_2$	PtCo-NPSC	39
Zn-air	300	10	6 M KOH + 0.2 M $Zn(Ac)_2$	Fe-NC HDAC + RuO_2	40
Zn-Air	500	10	6 M KOH + 0.2 M $Zn(Ac)_2$	NPVG/P_ene-1	41
Zn-air	330	10	6 M KOH + 0.2 M $Zn(Ac)_2$	Co-SAs/NVPC	42
Zn-air	100	10	6 M KOH + 0.2 M $Zn(Ac)_2$	Co_9S_8/CoS@ NSC	43
Zn-air	100	5	6 M KOH + 0.2 M $Zn(Ac)_2$	Co@N-CNT/ N-GY	44
Zn-air	170	10	6 M KOH + 0.2 M $Zn(Ac)_2$	Co/Co_9S_8/NC	45
Zn-air	330	5	6 M KOH + 0.2 M $Zn(Ac)_2$	Fe_3C@NSC	46
Zn-air	550	5	6 M KOH + 0.2 M $Zn(Ac)_2$	IrFe-SACs	47
Zn-air	1000	5	6 M KOH + 0.2 M $Zn(Ac)_2$	Fe_3O_4@NC/ FeCuN	48
Zn-air	1350	5	6 M KOH + 0.2 M $Zn(Ac)_2$	FeNi/ FeNiO-NCS	49

Table S5 Comparison of cycle stability of reported hybrid Zn batteries

Batteries	Cycle time (h)	Current density (mA cm^{-2})	Electrolyte	Cathode	Ref.
Zn-MnO_2/air	278	5	6 KOH + 0.2 $Zn(Ac)_2$ // 0.5 M K_2SO_4 // 3 M H_2SO_4 + 1 M $MnSO_4$	carbon felt	This work
Zn-Ag/air	10	1	6 KOH+0.2 M $Zn(Ac)_2$	Ag/RuO_2/CNT	50
Zn-Co_3O_4/air	440	10	6 M KOH and 0.2 M $Zn(AC)_2$	Co_3O_4 on CFC	51
Zn-Ag/Air	551	10	6 M KOH and 0.2 M $Zn(AC)_2$	Ag/stainless steel	52
Zn-Co_3O_4/air	100	10	6 M KOH and 0.2 M $Zn(AC)_2$	Co_3O_4/carbon cloth	53
Zn-Co_3O_4/air	330	10	6 M KOH and 0.1 M $Zn(AC)_2$	Co_3O_4/Ni foam	54
Zn-$NiCo_2S_4$/ Air	400	5	4 M KOH and 0.2 M $Zn(AC)_2$	$NiCo_2S_4$/ 3DNCC	55
Zn-Ni_3S_2/air	33	10	6 M KOH and 0.2 M $Zn(AC)_2$	Ni@Ni_3S_2	56
Zn-Co_3O_4/air	300	1	4.0 M KOH	O−Co_3O_4@ MCN	57
quasi-neutral Zn-MnO_2/air	1350	5	2 M NH_4Cl + 0.2 M $ZnCl_2$ + 0.02 M $MnSO_4$	PMO/N-rGO	58
Zn-$Co_{3-x}Ni_xO_4$/ air	200	5	KOH-PVA gel	NS@$Co_{3-x}Ni_xO_4$/Co_3O_4	59
Zn-Cu/Ni/air	500	5	6 M KOH + 0.2 M $Zn(AC)_2$	Cu_XO@NiFe-LDH/Co-N-C	60
Zn-Ni/air	400	2	3.5 g ZnO + 0.18 g LiOH + 100 g 30 wt.% KOH	$NiCo_2O_4$/N-G	61
Zn-Co/air	700	20	6 M KOH / 0.2 M $Zn(AC)_2$	Co/Co_2P@ PNCF	62
neutral Zn-Air/MnO_2	100	1	1 M $ZnSO_4$ + 0.1 M $MnSO_4$	CNTs/carbon paper	63
Zn-Ni/air	2500	5	6 M KOH / 0.2 M $Zn(AC)_2$	$NiCo_2O_4$/ NiF@C	64

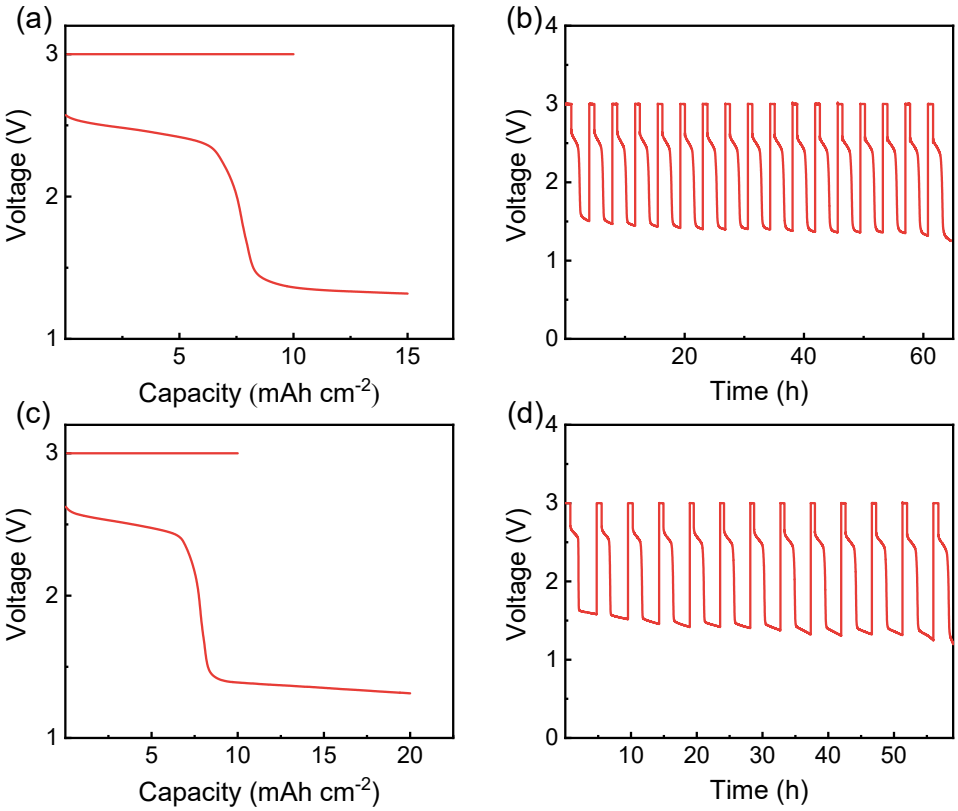

Fig. S10 Cycle stability of Zn-MnO_2/air battery with 10 mAh cm^{-2} charge and different discharge capacity at 5 mA cm^{-2}. (a, b) Discharge to 15 mAh cm^{-2}; (c, d) Discharge to 20 mAh cm^{-2}.

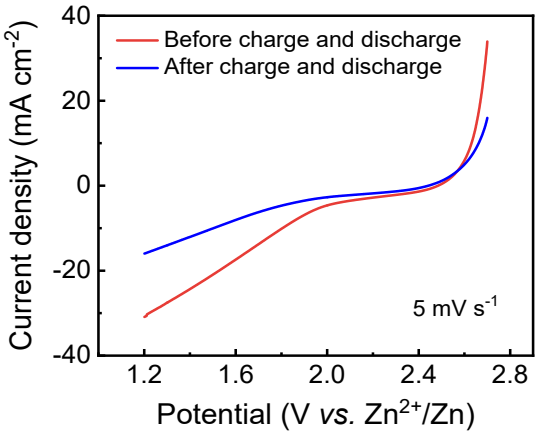

Fig. S11 (a) Comparison of ORR reduction current before and after charge and discharge.

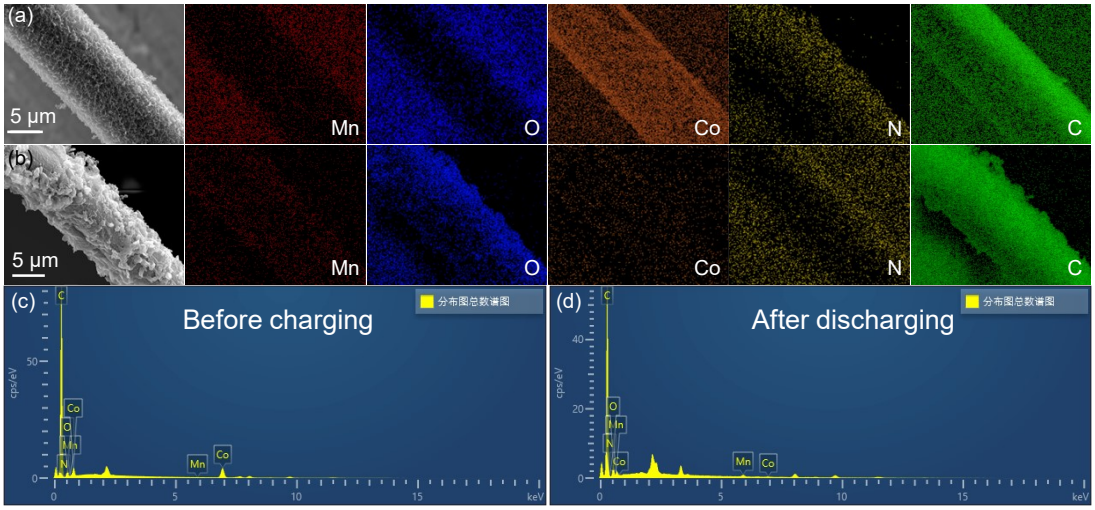

Fig. S12 (a, b) SEM and mapping comparison of electrodes of hybrid battery after charging of 10 mAh cm^{-2} and completely discharging of 25 mAh cm^{-2} at 2 mA cm^{-2} current density. (c, d) EDS of C@Co-N-C electrode assemble in Zn-MnO_2/air battery before charging and after discharging.

Table S6 Comparison of element content on Co-N-C electrode before charging and after discharging

Element	Before charging (Wt%)	After discharging (Wt%)
C	89.59	86.39
N	0.00	0.00
O	7.32	13.11
Mn	0.00	0.38
Co	3.08	0.12

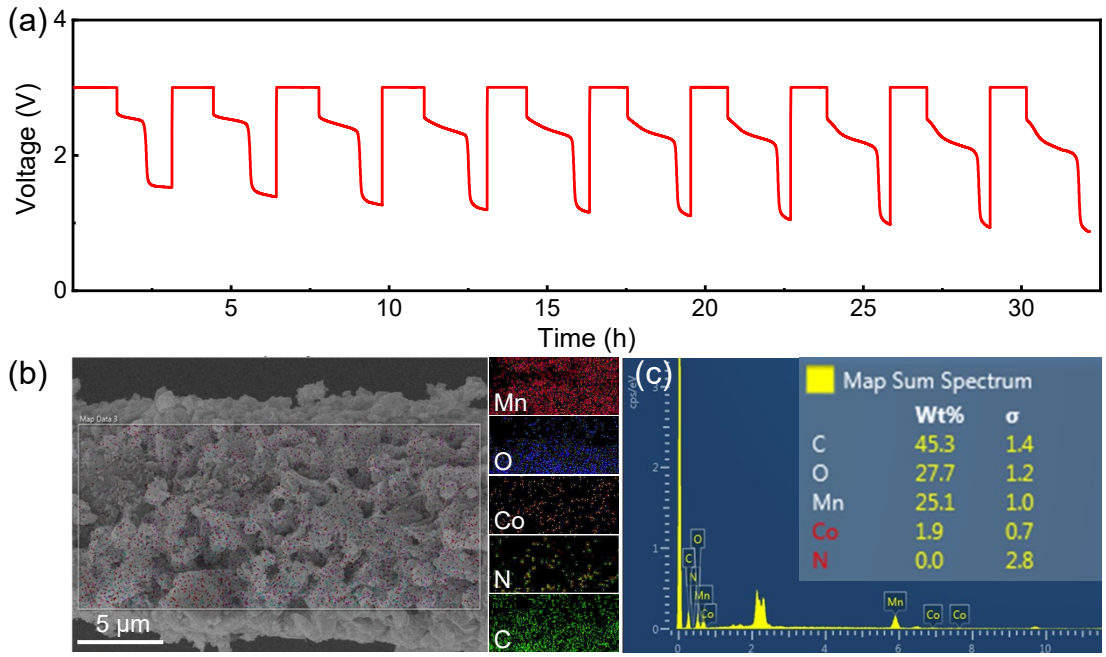

Fig. S13 (a) Time-voltage profiles of the Zn-MnO_2/air composite battery over 10 cycles with charge to 10 mAh cm^{-2} and discharge to 10 mAh cm^{-2} at 5 mA cm^{-2}; (b) SEM images of the multifunctional electrode after 10 cycles, together with elemental mapping of the selected regions; (c) EDS spectra of the cycled electrode and the corresponding elemental composition.

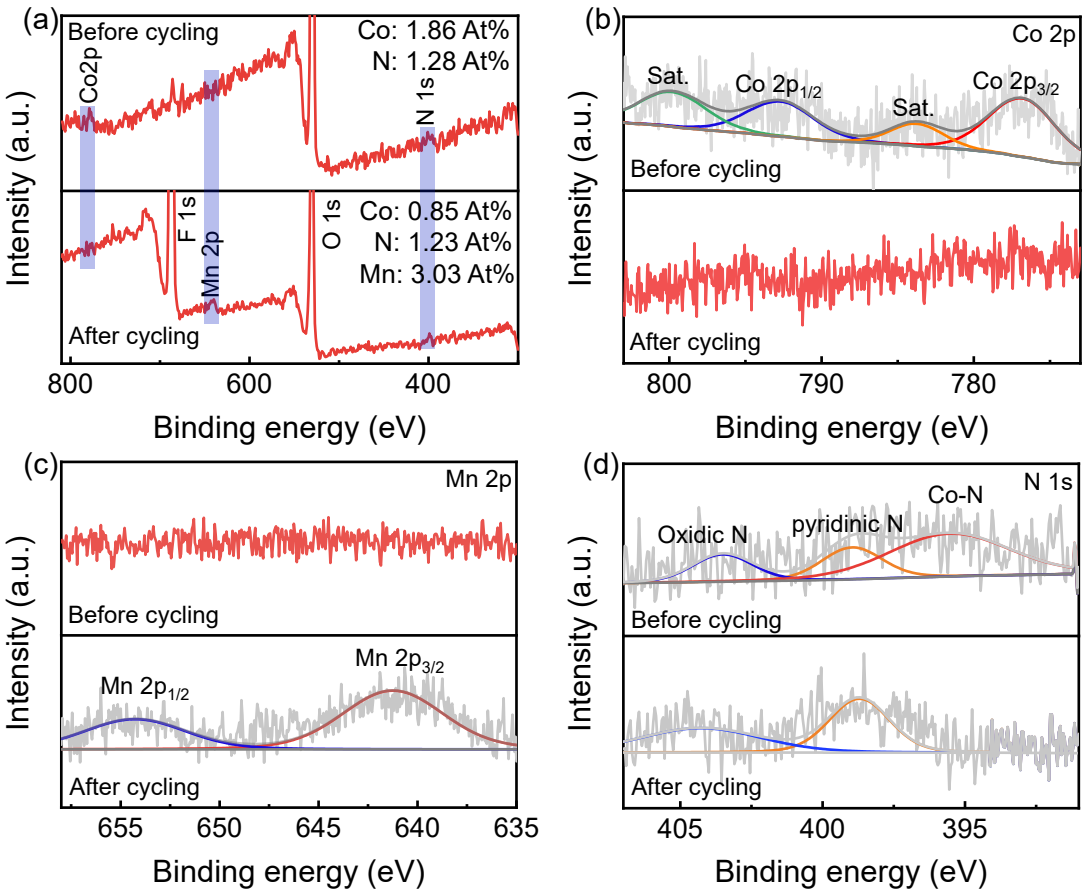

Fig. S14 XPS of C@Co-N-C electrode before and after 10 cycles with charge to 10 mAh cm^{-2} and discharge to 10 mAh cm^{-2} at 5 mA cm^{-2}. (a) A survey scan; (b) Co 2p; (c) Mn 2p; (d) N 1s.

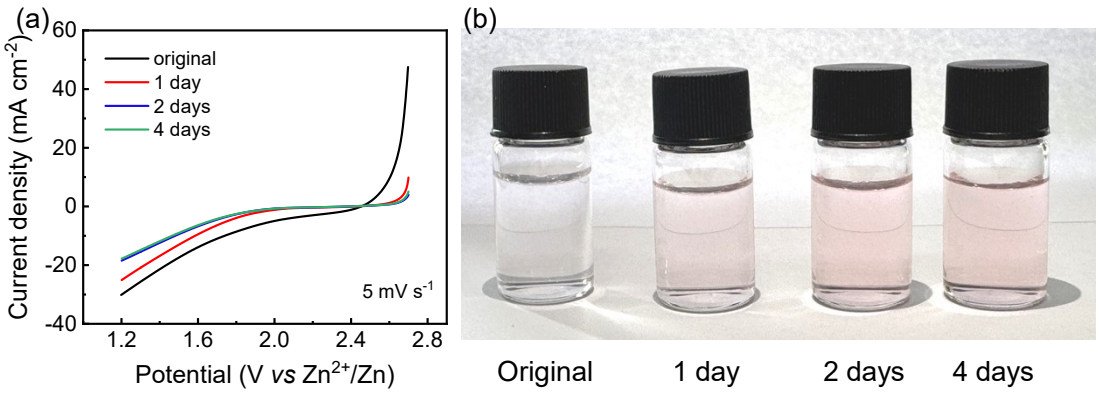

Fig. S15 Comparison of performance (a) and color changes (b) of the C@Co-N-C electrode in the battery after different storage periods.

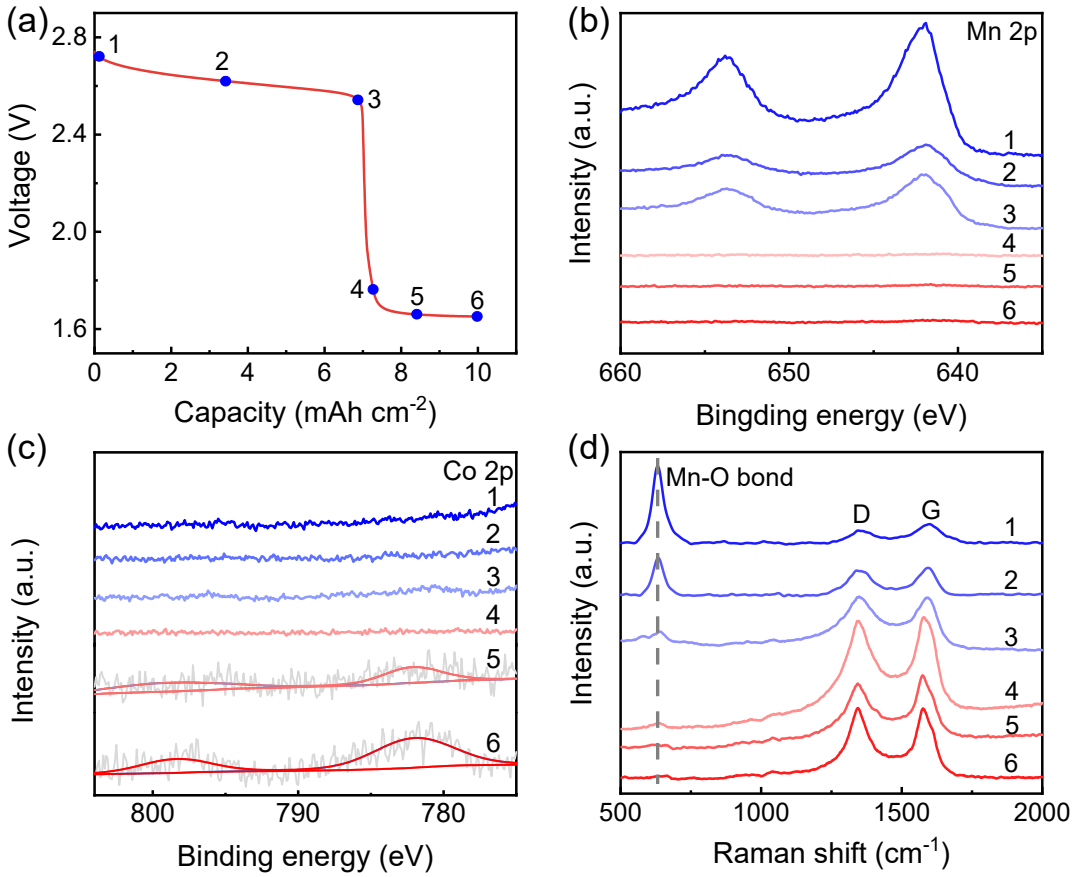

Fig. S16 (a) Discharge curve of hybrid Zn-MnO_2/air battery at a charge capacity of 10 mAh cm^{-2}. *Ex-situ* XPS of Mn 2p (b), Co 2p (c) and Raman curves (d) of at different discharge voltage in (a) (1: initial stage, 2.72 V; 2: 2.62 V; 3: 2.56 V; 4: 1.75 V; 5: 1.66 V; 6: 1.65 V).

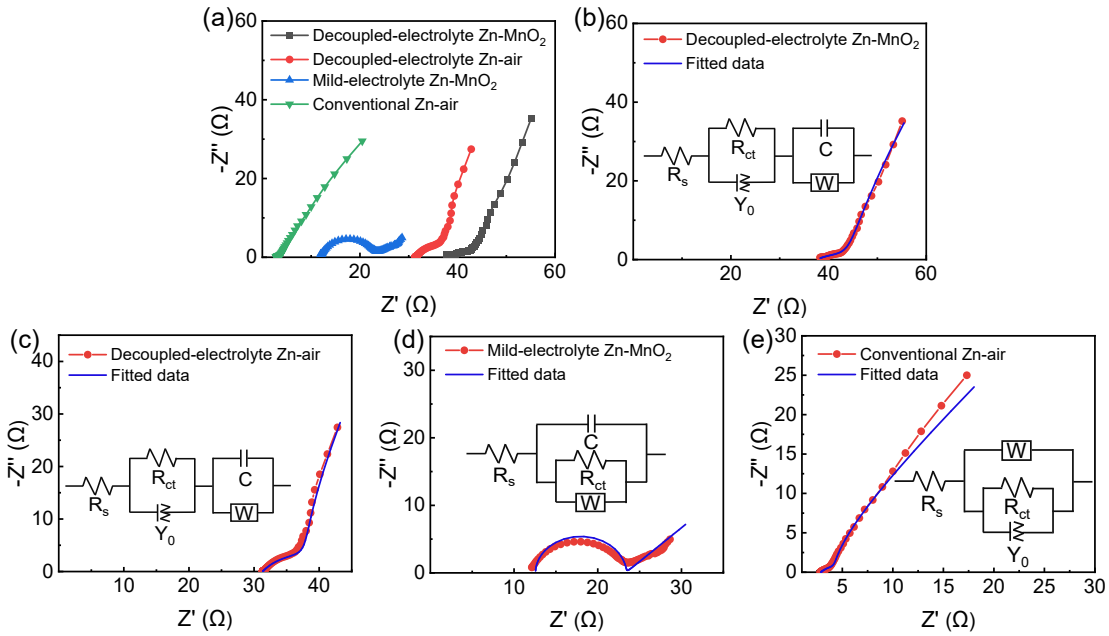

Fig. S17 (a) Nyquist plots of decoupled electrolyte Zn-MnO_2 batteries, decoupled electrolyte Zn-air batteries, mild electrolyte Zn-MnO_2 batteries and conventional Zn-air batteries; (b) Nyquist plots and fitted data of decoupled electrolyte Zn-MnO_2 batteries; (c) Nyquist plots and fitted data of decoupled electrolyte Zn-air batteries; (d) Nyquist plots and fitted data of mild electrolyte Zn-MnO_2 batteries; (e) Nyquist plots and fitted data of conventional Zn-air batteries.

References

1 B. Jiang, Y. He, B. Li, S. Zhao, S. Wang, Y.-B. He and Z. Lin, *Angew. Chem. Int. Ed.*, 2017, **56**, 1869-1872.

2 C. Guan, X. Liu, W. Ren, X. Li, C. Cheng and J. Wang, *Adv. Energy Mater.*, 2017, **7**, 1602391.

3 S. M. Hosseini, E. Jashni, S. Amani and B. Van der Bruggen, *J. Colloid Interface Sci.*, 2017, **505**, 763-775.

4 T. Luo, S. Abdu and M. Wessling, *J. Membr. Sci.*, 2018, **555**, 429-454.

5 D. Chao, C. Ye, F. Xie, W. Zhou, Q. Zhang, Q. Gu, K. Davey, L. Gu and S. Z. Qiao, *Adv. Mater.*, 2020, **32**, 2001894.

6 C. Liu, X. Chi, Q. Han and Y. Liu, *Adv. Energy Mater.*, 2020, **10**, 1903589.

7 C. Liu, X. Chi, C. Yang and Y. Liu, *Energy Environ. Mater.*, 2022, **6**, e12300.

8 X. Shen, X. Wang, Y. Zhou, Y. Shi, L. Zhao, H. Jin, J. Di and Q. Li, *Adv. Funct. Mater.*, 2021, **31**, 2101579.

9 Z. Liu, Y. Yang, S. Liang, B. Lu and J. Zhou, *Small Struct.*, 2021, **2**, 2100119.

10 J. Lei, Y. Yao, Z. Wang and Y. C. Lu, *Energy Environ. Sci.*, 2021, **14**, 4418-4426.

11 R. Liang, J. Fu, Y.-P. Deng, Y. Pei, M. Zhang, A. Yu and Z. Chen, *Energy Storage Mater.*, 2021, **36**, 478-484.

12 X. Zheng, Y. Wang, Y. Xu, T. Ahmad, Y. Yuan, J. Sun, R. Luo, M. Wang, M. Chuai, N. Chen, T. Jiang, S. Liu and W. Chen, *Nano Lett.*, 2021, **21**, 8863-8871.

13 X. Zheng, R. Luo, T. Ahmad, J. Sun, S. Liu, N. Chen, M. Wang, Y. Yuan, M. Chuai, Y. Xu, T. Jiang and W. Chen, *Energy Environ. Mater.*, 2023, **6**, e12433.

14 Z. Shen, Y. Liu, L. Luo, J. Pu, Y. Ji, J. Xie, L. Li, C. Li, Y. Yao and G. Hong, *Small*, 2022, **18**, 2204683.

15 S. Gao, B. Li, H. Tan, F. Xia, O. Dahunsi, W. Xu, Y. Liu, R. Wang and Y. Cheng, *Adv. Mater.*, 2022, **34**, 2201510.

16 Y. Cui, Z. Zhuang, Z. Xie, R. Cao, Q. Hao, N. Zhang, W. Liu, Y. Zhu and G. Huang, *ACS Nano*, 2022, **16**, 20730-20738.

17 C. Xie, T. Li, C. Deng, Y. Song, H. Zhang and X. Li, *Energy Environ. Sci.*, 2020, **13**, 135-143.

18 Y. Liu, Z. Qin, X. Yang, J. Liu, X. X. Liu and X. Sun, *ACS Energy Lett.*, 2022, **7**, 1814-1819.

19 P. Ruan, X. Chen, L. Qin, Y. Tang, B. Lu, Z. Zeng, S. Liang and J. Zhou, *Adv. Mater.*, 2023, **35**,

2300577.

20 X. Xue, Z. Liu, S. Eisenberg, Q. Ren, D. Lin, E. Coester, H. Zhang, J. Z. Zhang, X. Wang and Y. Li, *ACS Energy Lett.*, 2023, **8**, 4658-4665.

21 Q. Chen, J. Li, C. Liao, W. Liang, X. Lou, Z. Liu, J. Zhang, Y. Tang, L. Mai, L. Zhou and K. Amine, *Nano Energy*, 2024, **126**, 109607.

22 Q. Wang, W. Zhou, Y. Zhang, H. Jin, X. Li, T. Zhang, B. Wang, R. Zhao, J. Zhang, W. Li, Y. Qiao, C. Jia, D. Zhao and D. Chao, *Natl. Sci. Rev.*, 2024, **11**, nwae230.

23 Y. Liu, C. Xie and X. Li, *Small*, 2024, **20**, 2402026.

24 X. Xue, Z. Liu, S. Chandrasekaran, S. Eisenberg, C. Althaus, M. C. Freyman, A. Pinongcos, Q. Ren, L. Valdovinos, C. Hsieh, B. Hu, B. Dunn, C. A. Orme, X. Wang, M. A. Worsley and Y. Li, *Adv. Mater.*, 2025, **37**, 2419505.

25 Y. Wang, H. Hong, Z. Wei, D. Li, X. Yang, J. Zhu, P. Li, S. Wang and C. Zhi, *Energy Environ. Sci.*, 2025, **18**, 1524-1532.

26 D. Chao, W. Zhou, C. Ye, Q. Zhang, Y. Chen, L. Gu, K. Davey and S.-Z. Qiao, *Angew. Chem. Int. Ed.*, 2019, **58**, 7823-7828.

27 M. Chuai, H. Tong, Z. Yang, S. Deng, M. Wu, J. Xing and G. Chai, *J. Am. Chem. Soc.*, 2025, **147**, 31591-31602.

28 W. Fan, S. Tian, L. Qin, T. S. Alomar, P. Ruan, Z. M. El-Bahy, N. AlMasoud, B. Lu and J. Zhou, *J. Am. Chem. Soc.*, 2025, **147**, 18694-18703.

29 H. Chen, P. Ruan, H. Zhang, Z. M. El-Bahy, M. M. Ibrahim, B. Lu and J. Zhou, *Angew. Chem. Int. Ed.*, 2025, **64**, e202423999.

30 R. Liu, C. Wang, F. Wan, K. Hu, D. Yang, Y. Xia, W. Yin, Y. Lin, Y. Chen, S. Sun and W. Chen, *Adv. Funct. Mater.*, 2025, **36**, e17166.

31 M. Zhang, T. Xu, W. Liu, H. Zhang, J. Qi, X. Wang, Y. Wang, L. Zhu, K. Liu, J. Wang and C. Si, *Carbon Energy*, 2025, e70097.

32 S. Liu, D. Jiang, N. Lu, L. Li, Z. Zhang, G. Kang, S. Wang and G. Wang, *ACS Appl. Mater. Interfaces*, 2025, **17**, 69449-69457.

33 Q. Li, M. Xu, S. Wei, A. Kumar, K. K. Abdalla, Y. Wang, L. Yu, M. Liu, X. Jin, J. Li, L. Song, Y. Zhao and X. Sun, *Energy Environ. Sci.*, 2025, **18**, 7939-7949.

34 W. Zhuang, Z. Wang, C. Li, K. Zhang, X. Chen, L. Lin, Z. Shao, W. Wang, Y. Tan, S. Cheng, R. Lin,

G. Hong and Y. Yao, *Adv. Mater.*, 2026, **38**, e22827.

35 K. Chen, R. Li, S. Zhang, Y. Li, B. Guo, X. Wang and Y. Liu, *Chem. Eng. J.*, 2026, **530**, 173494.

36 Y. Hu, D. Zhang, Z. Liu, H. He, H. Wang, C. Deng and S. Zhang, *J. Colloid Interface Sci.*, 2026, **704**, 139462.

37 J. Wei, L. Tan, Q. Ma, X. Long, S. Li, Y. Shi, R. Gao, Z. Xu, D. Luo, J. Zhang, D. Li, X. Wang, A. Yu and Z. Chen, *Nano-Micro Lett.*, 2026, **18**, 124.

38 J. Li, C. Li, B. Liu, Y. Li, O. Borodin and L. F. Nazar, *Nat. Energy*, 2026, **11**, 299-312.

39 Y. Ma, L. Li, Q. Liu, W. Yang, X. Cao, Y. He, J. Wang, Z. Li and L. Wang, *ACS Sustain. Chem. Eng.*, 2026, **14**, 5076-5087.

40 D. Kim, S. Jung, G. Park, M.-j. Song, D. Lee, J. Y. Lee, H. Choi, J. Kim, Y. Shin, J. Na, H. Lim, S. Oh, S.-M. Bak and J. Kim, *Applied Catalysis B: Environment and Energy*, 2026, **390**, 126624.

41 Z. Wu, G. Zhang, X. Zuo, H. Ba, Y. Yu, Y. Shen and G. Shao, *Applied Catalysis B: Environment and Energy*, 2026, **391**, 126665.

42 H. Pan, M. Li, J. Liu, Q. Li, J. Wu, L. Tian, X. Huang, J. Yu, H. Li, J. Dou and X. Chen, *J. Colloid Interface Sci.*, 2026, **713**, 140178.

43 H. Lee, B. Lee, J. Shin, K. Min and S.-H. Baeck, *Journal of Energy Storage*, 2026, **154**, 121213.

44 M. Zeng, H. Shi, W. Cui, X. Wu, S. Liang, W. Wang, N. Akbarjon and Z. Xu, *J. Alloys Comp.*, 2026, **1061**, 187371.

45 Y.-N. Chen, W. Liao, S. Yao, C. Wang, Z. Liu, L. E, D. Zhao, J. Li, W. Ding, H. Zhang and S. Wu, *J. Alloys Comp.*, 2026, **1060**, 187320.

46 S. Guo and B. Hui, *Mater. Today Energy*, 2026, **58**, 102264.

47 Y. Tan, A. Li, Y. Wang, X. Jiang, Y. Cheng, D. Chao, Y. Zhang and C. Cheng, *Nano-Micro Lett.*, 2026, **18**, 272.

48 G. L. Li, L. Xu, F. Jiang, Q. Zhuo, C. Jin, X. L. Zhang, Y. Yan, N. Gao and Q. Mao, *Small*, 2026, **0**, e12895.

49 R. Xin, H. Zhao, Y. Liu, Y. Yuan, S. Liu, D. Li, M. Yang, B. Liu, S. Ding and Z. Lin, *Adv. Funct. Mater.*, 2025, e24205.

50 P. Tan, B. Chen, H. Xu, W. Cai, W. He, H. Zhang, M. Liu, Z. Shao and M. Ni, *ACS Appl. Mater. Interfaces*, 2018, **10**, 36873-36881.

51 L. Ma, S. Chen, Z. Pei, H. Li, Z. Wang, Z. Liu, Z. Tang, J. A. Zapien and C. Zhi, *ACS Nano*, 2018,

12, 8597-8605.

52 C.-C. Chang, Y.-C. Lee, H.-J. Liao, Y.-T. Kao, J.-Y. An and D.-Y. Wang, *ACS Sustain. Chem. Eng.*, 2018, **7**, 2860-2866.

53 P. Tan, B. Chen, H. Xu, W. Cai, W. He, M. Liu, Z. Shao and M. Ni, *Small*, 2018, **14**, 1800225.

54 P. Tan, B. Chen, H. Xu, W. Cai, W. He and M. Ni, *Appl. Catal. B Environ.*, 2019, **241**, 104-112.

55 X. Wang, X. Xu, J. Chen and Q. Wang, *ACS Sustain. Chem. Eng.*, 2019, **7**, 12331-12339.

56 Z. Huang, X. Li, Q. Yang, L. Ma, F. Mo, G. Liang, D. Wang, Z. Liu, H. Li and C. Zhi, *J. Mater. Chem. A*, 2019, **7**, 18915-18924.

57 D. Xu, S. Wu, X. Xu and Q. Wang, *ACS Sustain. Chem. Eng.*, 2020, **8**, 4384-4391.

58 T. Zhang, S. Zhang, S. Cao, Q. Yao and J. Y. Lee, *Energy Storage Mater.*, 2020, **33**, 181-187.

59 M. Wu, G. Zhang, N. Chen, W. Chen, J. Qiao and S. Sun, *Energy Storage Mater.*, 2020, **24**, 272–280.

60 G. Zhang, X. Liu, L. Wang, G. Xing, C. Tian and H. Fu, *ACS Nano*, 2022, **16**, 17139-17148.

61 Y. Ma, Z. Zhao, Y. Cui, J. Yu and P. Tan, *Small*, 2023, **20**, 2308500.

62 Z. Xu, J. Chen, T. Zhang, H. Lu, L. Yan, J. Ning and Y. Hu, *Adv. Energy Mater.*, 2024, **15**, 2402839.

63 Y. Feng, S. Luo, A. Duan, M. Li, B. Zhang and W. Sun, *Adv. Energy Mater.*, 2025, 2501294.

64 B. Li, J. Quan, A. Loh, J. Chai, Y. Chen, C. Tan, X. Ge, T. S. A. Hor, Z. Liu, H. Zhang and Y. Zong, *Nano Lett.*, 2016, **17**, 156-163.